JOURNAL OF VIROLOGY, Oct. 1995, p. 6487–6497 Vol. 69, No. 10
0022-538X/95/$04.00+0
Copyright © 1995, American Society for Microbiology

Self-Assembly In Vitro of Purified CA-NC Proteins from Rous Sarcoma Virus and Human Immunodeficiency Virus Type 1

STEPHEN CAMPBELL AND VOLKER M. VOGT*

Section of Biochemistry, Molecular and Cell Biology, Cornell University, Ithaca, New York 14853

Received 15 May 1995/Accepted 19 July 1995

The internal structural proteins of retroviruses are proteolytically processed from the Gag polyprotein, which alone is able to assemble into virus-like particles when expressed in cells. All Gag proteins contain domains corresponding to the three structural proteins MA, CA, and NC. We have expressed the CA and NC domains together as a unit in *Escherichia coli*, both for Rous sarcoma virus (RSV) and for human immunodeficiency virus type 1 (HIV-1). We also expressed a similar HIV-1 protein carrying the C-terminal p6 domain. RSV CA-NC, HIV-1 CA-NC, and HIV-1 CA-NC-p6 were purified in native form by classic methods. After adjustment of the pH and salt concentration, each of these proteins was found to assemble at a low level of efficiency into structures that resembled circular sheets and roughly spherical particles. The presence of RNA dramatically increased the efficiency of assembly, and in this case all three proteins formed hollow, cylindrical particles whose lengths were determined by the size of the RNA. The optimal pH at which assembly occurred was 5.5 for the RSV protein and 8.0 for the HIV-1 proteins. The treatment of the RSV CA-NC cylindrical particles with nonionic detergent, with ribonuclease, or with viral protease caused disassembly. These results suggest that RNA plays an important structural role in the virion and that it may initiate and organize the assembly process. The in vitro system described should facilitate the dissection of assembly pathways in retroviruses.

The macromolecular interactions involved in the assembly of retroviruses within the infected cell are poorly understood. In this process viral proteins must interact with each other, with the RNA genome, with the plasma membrane, and at least in some cases with cellular proteins. Retroviruses are classified in part by their pathway of assembly. Type C retroviruses, such as the avian sarcoma and leukemia viruses (whose prototype is Rous sarcoma virus [RSV]), and lentiviruses, such as human immunodeficiency virus type 1 (HIV-1), form at the plasma membrane and bud outward into the extracellular space. The first step in this process that is visible by electron microscopy (EM) is the appearance of small, flat patches of electron-dense material beneath the plasma membrane. As these patches enlarge, they acquire curvature to produce first a shallow crescent shape and eventually a spherical bud connected to the cell by a thin stalk. The bud finally pinches off and is released. At some point during this series of steps the budding virion acquires its envelope proteins and two copies of the viral RNA genome. It is not known whether these events occur sequentially or simultaneously. It is possible that the viral proteins and RNA form a loosely organized and invisible complex prior to membrane association. Alternatively, the individual components may each be transported to the plasma membrane separately and then somehow colocalize at the site of assembly. Type B and type D retroviruses (whose prototypes are mouse mammary tumors virus and Mason-Pfizer monkey virus [M-PMV], respectively) first form the virus core within the cytoplasm, which then is transported as a particle to the plasma membrane where it is enveloped by budding. For these retroviruses, assembly and budding are distinct processes.

The information required to form a budding virus-like particle is contained entirely within the viral Gag protein, the polyprotein precursor from which the mature internal structural proteins are derived by proteolytic cleavage. The viral protease (PR) is activated to process Gag late in assembly. In RSV the domains in Gag corresponding to the mature proteins are, from N terminus to C terminus, MA (matrix), p2, p10, CA (capsid), NC (nucleocapsid), and PR. In HIV-1 the Gag domains are MA, CA, NC, and p6. The MA domain is involved in the association of Gag with the plasma membrane, both in RSV (48–50, 68, 70) and in HIV-1 (4, 19, 21, 75). The functions of the RSV p2 and p10 domains and the HIV-1 p6 domain are poorly understood, but portions of these polypeptide segments may play a role in the release of the budding virus from the plasma membrane (25, 46, 69). The role of the CA domain in assembly is uncertain. In an overexpression system for RSV Gag, large deletions that additively encompass all of CA can be tolerated without significantly reducing the ability of Gag to assemble and be released as particles into the medium. However, in some cases the virus-like particles produced by these deletion mutants are heterogeneous in size, suggesting that CA may have a role in determining virion size (68). In HIV-1, the CA domain appears to be more sensitive to mutation. Some deletions or linker insertions have little or no effect on assembly (11, 14, 64, 65), while others prevent assembly (11, 14, 74) or alter the size of the particles (11, 14). As a mature protein, CA is believed to form a shell around the viral nucleoprotein core. In RSV this shell is roughly spherical, while in HIV-1 it is conical in shape. The NC domain packages and protects the viral RNA genome within the nucleoprotein core. HIV-1 NC has been shown to specifically bind to HIV-1 RNA in vitro (5, 6, 12, 63). No such specificity in RNA binding has yet been shown for RSV NC. In both RSV and HIV-1 the NC domain contains two copies of a conserved cysteine-histidine box motif, $C\text{-}X_2\text{-}C\text{-}X_4\text{-}H\text{-}X_4\text{-}C$, with a flanking stretch of basic residues. Mutational analyses of this motif and basic residues suggested that the motif is essential for encapsidation of genomic RNA (7, 12, 15, 16, 23, 24, 43).

Mutational analyses of the RSV Gag protein have indicated that only three small regions, called assembly domains (AD), are essential for the budding of virus-like particles from cells

* Corresponding author. Mailing address: Section of Biochemistry, Molecular and Cell Biology, Biotechnology Building, Cornell University, Ithaca, NY 14853. Phone: (607) 255-2443. Fax: (607) 255-2428. Electronic mail address: vmv1@cornell.edu.

transfected with the *gag* gene. AD1 is located at the amino terminus of Gag within MA and is involved in membrane binding (4, 71, 75). AD2 is located within p2 and appears to be required for the last steps in budding (69). AD3 is present as two redundant copies within NC. This AD appears to be required for productive interactions between Gag molecules during assembly (53, 68). This conclusion is derived from the observation that RSV Gag mutants carrying AD3, even if AD1 or AD2 is deleted, can be incorporated efficiently into particles when coexpressed with wild-type Gag, while deletion mutants lacking AD3 cannot be rescued in this manner (70). Chimeras between RSV and HIV-1 Gag (4) and deletions within HIV-1 Gag (10, 25, 36, 75) have identified similar AD in HIV-1. Of particular relevance to the results presented below is the report that HIV-1 Gag protein with the entire MA domain deleted assembles into virus-like particles in transfected cells, if the amino terminus of CA is mutated so that the truncated Gag protein becomes myristylated (36).

We reasoned that if AD3 is responsible for Gag-Gag interactions, fragments of Gag containing AD3 might be able to assemble in vitro as purified proteins into virus-like particles. We present evidence that CA-NC from RSV as well as CA-NC and CA-NC-p6 from HIV-1, after purification without denaturation from an *Escherichia coli* expression system, can form particles when the pH and ionic strength are adjusted to appropriate values. The addition of RNA to the reaction mixture greatly increases the level of assembly efficiency but alters the morphology of the resulting particles so that they are cylindrical. From the appearance of the CA-NC-RNA particles in negative-stain and thin-section EM, we suggest a model for the assembly.

MATERIALS AND METHODS

DNA constructs. All plasmids were constructed by using common subcloning techniques and propagated in the DH5α strain of *E. coli*. After confirmation by restriction digestion, the plasmids were moved into the BL21 DE3 pLys S strain of *E. coli* for protein expression. Nucleotides of the RSV genome are numbered as described in the original sequence of the PrC strain of RSV (55). The plasmid pSXK.PR-L1* has been described previously (59). Two intermediate constructs were created. The expression vector pET 3xc (Novagen) was cut with *Nde*I (at nucleotide [nt] 1294), blunt ended with S1 nuclease, cut with *Bam*HI (at nt 510), and ligated to the *Bal*I-*Bam*HI (nt 1089 to 1916) sequence from pSXK.PR-L1* to create pET 3xc CA-N. The other intermediate construct, pET 3xc A-NC, was generated by replacing the *Nde*I-*Kpn*I sequence of pET 3xc (nt 1294 to 520) with the *Nde*I-*Kpn*I sequences from pSXK.PR-L1* (nt 1290 to 4995). Both of the intermediate constructs share a *Sac*II site (at nt 1806) from the RSV sequence. The *Xba*I (nt 1332 in pET 3xc)-*Sac*II (nt 1806 in RSV) sequence of pET 3xc A-NC was replaced with the *Xba*I-*Sac*II sequence from pET 3xc CA-N to create pET 3xc CA-NC.

For expression of HIV CA-NC and CA-NC-p6, these segments of the *gag* gene of HIV-1 strain BH10 were amplified with primers carrying an *Nde*I site and an ATG initiation codon (5′ primer), or carrying a *Kpn*I (3′ primer). For the CA-NC-p6 construct, the 3′ primer was positioned downstream of the normal termination codon at the end of *gag*. For the CA-NC construct, a codon for leucine was replaced by a termination codon immediately following the amino acid sequence RPGNF.

Protein expression and purification. *E. coli* BL21 DE3 cells were grown and induced for protein expression as previously described (61, 62). An overnight culture was inoculated at 1:100 and grown for 2 h at 37°C with shaking. To induce protein expression, IPTG (isopropyl-β-D-thiogalactopyranoside) was added to 0.4 mM, and an extra 20 μg of ampicillin per ml was added. Four hours later the cells were harvested by centrifugation and frozen at −20°C.

Purification of RSV CA-NC and HIV-1 CA-NC and CA-NC-p6 was modified from the method of Pognonec et al. (51). The frozen bacterial pellet was resuspended on ice in buffer A (20 mM Tris [pH 7.5], 10% glycerol, 1 mM EDTA, 1 mM phenylmethylsulfonyl fluoride, 10 mM dithiothreitol) plus 0.5 M NaCl, at 25 ml/liter of cell culture. The cells were broken by sonication. Insoluble debris was removed by centrifugation, and soluble protein was precipitated with 25% saturated ammonium sulfate. The precipitate was resuspended in buffer A plus 0.5 M NaCl but without glycerol, at 2 ml/liter of cell culture, and incubated on ice for 30 min. Buffer A was slowly added until the final NaCl concentration was 0.1 M. Insoluble protein was removed by centrifugation, and the supernatant was mixed with phosphocellulose (Whatman P11) at a ratio of 10:1. The resin with bound protein was washed with buffer A plus 0.1 M NaCl and then with buffer A plus 0.3 M NaCl. The volumes of the washes were approximately 3 ml/ml of packed resin. CA-NC was eluted with buffer A plus 0.5 M NaCl. In some experiments a second elution was carried out with buffer A plus 1.0 M NaCl, which yielded additional CA-NC. The eluted protein was precipitated with 50% ammonium sulfate, resuspended in buffer A plus 0.5 M NaCl at 10 mg of protein per ml, and dialyzed at 4°C overnight against the same buffer.

Mature RSV CA and NC proteins were purified from RSV CA-NC that had been digested with avian myeloblastosis virus (AMV) PR, which had been purified from disrupted AMV particles by chloroform-methanol extraction (29). (AMV is a commercially available mixture of viruses, consisting primarily of myeloblastosis-associated viruses A and B, which have an approximate genome size of 7 kb). CA-NC in 50 mM MES [2-(*N*-morpholino)ethanesulfonic acid, pH 6]–0.8 M NaCl was digested overnight at 37°C with 0.1% (wt/wt) PR. The digested proteins were precipitated with ammonium sulfate to 50% saturation, dialyzed overnight against buffer A plus 100 mM NaCl, and mixed with phosphocellulose as described above. CA remained in the supernatant and was collected by precipitation with ammonium sulfate to 50% saturation and dialyzed overnight at 4°C against buffer A plus 0.5 M NaCl. NC was eluted from the resin with buffer A plus 0.5 M NaCl. All *E. coli*-expressed proteins were stored at 4°C. Protein concentration was determined by spectrophotometry and Coomassie blue staining after sodium dodecyl sulfate-polyacrylamide gel electrophoresis (SDS-PAGE).

Cross-linking and RNA purification. Proteins were incubated with either 1-ethyl-3-(3-dimethylaminopropyl)carbodiimide (EDC) (Pierce Chemical Company), which cross-links carboxyl to amino groups, or with dimethyl suberimidate (DMS) (Pierce Chemical Company), which cross-links primary amino groups. For cross-linking with EDC, the protein (10 mg/ml) was first dialyzed against a solution containing 50 mM MES (pH 5.5), 0.1 M NaCl, 1 mM EDTA, and 10 mM dithiothreitol. For cross-linking with DMS, 50 mM triethanolamine was used as a buffer. The bifunctional reagent was added to the indicated concentration, and the reaction mixture was incubated at room temperature for 2 h before quenching with 0.1 M glycine followed by SDS-PAGE.

Total *E. coli* RNA was purified as described in reference 2. RNA was synthesized in vitro by transcription with T7 RNA polymerase according to instructions from the manufacturer (Promega Corp.). Tobacco mosaic virus (TMV) and AMV RNA were purified by digesting purified virus with proteinase K in 1% SDS in 10 mM Tris-HCl (pH 8)–1 mM EDTA at 37°C for 1 h, after which phenol-chloroform extraction and ethanol precipitation were performed.

In vitro assembly and analysis by EM. Protein was diluted from 10 mg/ml to 1 mg/ml with storage buffer and dialyzed overnight at 4°C against the indicated buffers. When RNA was used in assembly it was added to the diluted protein prior to dialysis. Particles that formed under these conditions were negatively stained either with 2% uranyl acetate (pH 5) or phosphotungstic acid (pH 7.3) on Formvar carbon-coated grids. For thin sections, assembled particles first were collected by centrifugation for 1 h at 14,000 rpm in an Eppendorf microcentrifuge. HIV CA-NC and CA-NC-p6 pellets were fixed for 2 h in 0.1 M sodium cacodylate (pH 7.4)–3% glutaraldehyde. RSV CA-NC pellets were fixed for 2 h in 0.1 M sodium maleate (pH 5.2)–3% glutaraldehyde. After the fixation step both HIV and RSV particles were treated identically. Fixed pellets were washed in 0.1 M sodium cacodylate, pH 7.4, and then postfixed in 1% OsO_4 in the same buffer for 2 h at 4°C. The pellets then were rinsed in 0.1 M sodium maleate, pH 5.2, and stained with 1% uranyl acetate in 0.1 M sodium maleate, pH 6.0, for 1 h in the dark, rinsed again with sodium maleate, and dehydrated with ethanol before being embedded in Spur embedding media. Thin sections were counterstained with 2% uranyl acetate and lead citrate.

RESULTS

To be most useful, an in vitro viral assembly system requires large amounts of soluble protein. While unprocessed Gag polyproteins are difficult to purify in large quantities in a soluble form and without prior denaturation, the mature Gag proteins have proved to be more tractable (8, 17, 18, 41, 44, 52). We hypothesized that fragments of Gag consisting of more than one domain would retain assembly properties and yet be easier to purify. Since both the CA and NC domains are believed to be important in Gag-Gag interactions (for a review, see references 28 and 70), constructs were made for the expression of CA-NC in *E. coli*. Initial investigations focused on CA-NC from RSV, but they were extended to include CA-NC and CA-NC-p6 from HIV-1 to determine to what extent the observations might be generally valid for retroviruses.

The RSV CA-NC protein contains the complete CA and NC domains, including the spacer peptide between them (Fig. 1A). The amino acid sequence is identical to the sequence that corresponds to this segment of the authentic Gag protein, since

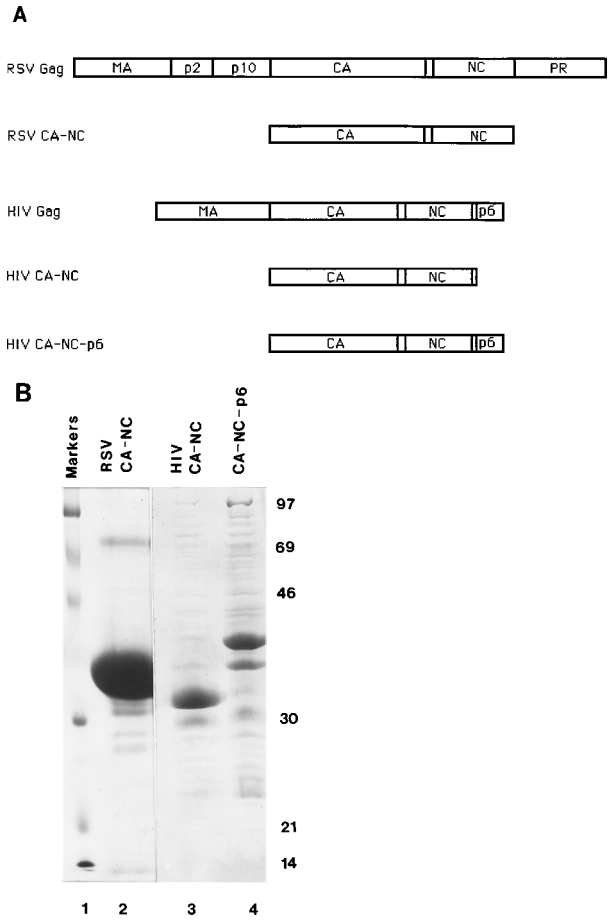

FIG. 1. Schematic diagram of RSV and HIV Gag proteins and purified proteins. (A) Schematic diagrams of the RSV and HIV Gag polyproteins are shown above their respective CA-NC and CA-NC-p6 fragments expressed in *E. coli* from the pET 3xc expression vector. RSV, Rous sarcoma virus. (B) Coomassie blue-stained SDS-polyacrylamide gel of purified proteins. Lane 1, molecular mass markers, with sizes in kilodaltons indicated to the right; lane 2, RSV CA-NC (200 μg); lane 3, HIV CA-NC; lane 4, HIV CA-NC-p6.

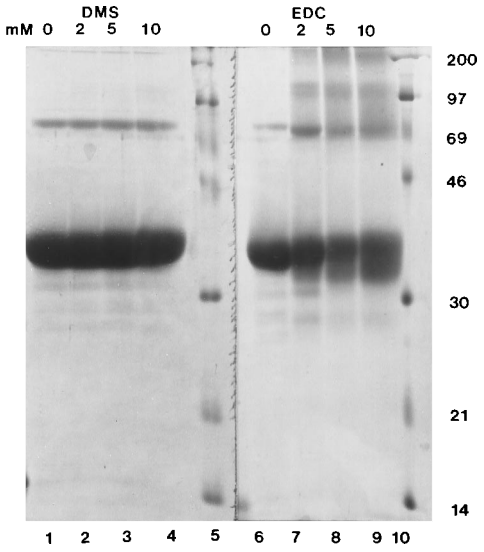

FIG. 2. Effect of cross-linking reagents on CA-NC. RSV CA-NC (1 mg/ml) was treated for 2 h at room temperature with DMS in triethanolamine, pH 8.2, or with EDC in MES, pH 5.5. Lane 1, no DMS; lane 2, 2 mM DMS; lane 3, 5 mM DMS; lane 4, 10 mM DMS; lane 6, no EDC; lane 7, 2 mM EDC; lane 8, 5 mM EDC; lane 9, 10 mM EDC; lanes 5 and 10, molecular weight markers.

the initiating methionine is removed in *E. coli* (48a) and the termination codon replaces the first amino acid of PR. We developed a rapid purification for this protein, based on ammonium sulfate precipitation and batch elution from phosphocellulose, which yielded RSV CA-NC, which was soluble at greater than 15 mg/ml in storage buffer and ca. 98% pure by densitometry of stained gels (Fig. 1B, lane 2). Identification of the purified protein was confirmed by migration on SDS-polyacrylamide gels, immunoblotting with anti-CA and anti-NC antisera, and digestion with PR to produce the correct mature CA and NC proteins (data not shown). An apparent contaminant was seen to migrate in SDS-polyacrylamide gels at 70 kDa, which is twice the size of RSV CA-NC. This protein could be removed by gel filtration, but it reappeared upon concentration of the RSV CA-NC fractions. It could be digested with PR and was recognized by both anti-CA and anti-NC antisera (data not shown). These results indicate that the 70-kDa band is a CA-NC dimer. Minor amounts of lower-molecular-mass polypeptides were visible in differing amounts in CA-NC preparations, and these were inferred to be degradation products, as indicated by their detection with the same antisera.

The HIV CA-NC and CA-NC-p6 constructs were similar in design to RSV CA-NC, but the initiating methionine was added by PCR (Fig. 1A). The expression and purification of the HIV proteins was the same as for RSV CA-NC, but the yields were lower, and as a consequence, the contaminating bacterial proteins represented a larger percentage of the final purified HIV proteins (Fig. 1B, lanes 3 and 4). The identity of the HIV proteins was also confirmed by immunoblotting and by digestion with HIV PR (data not shown).

The presence of an SDS-resistant dimer suggested that RSV CA-NC could multimerize in vitro. To further determine conditions that promote multimerization, we employed two chemical cross-linking reagents. DMS, which cross-links primary amines at an alkaline pH, has been used previously to cross-link MA, CA, and NC both in mature avian sarcoma and leukemia viruses and murine leukemia virus (MLV) (47–50), as well as unprocessed MA, CA, and NC domains from a PR-deficient strain of MLV (48). EDC cross-links carboxyl groups to amino groups at an acidic pH. Incubating RSV CA-NC, at a protein concentration of 1 mg/ml, with these reagents gave different results (Fig. 2). DMS did not produce cross-linked products at pH 8, which is within the range of 0 to 10 mM cross-linker. As a control to ensure that the reagent was functional, cross-linking of purified mature AMV under identical conditions showed the same dimers and multimers of CA as in previous reports (49) (data not shown). By contrast, EDC at pH 5.5 efficiently produced RSV CA-NC multimers (Fig. 2; compare lane 6 with lanes 7 to 9). Immunoblotting confirmed that these larger multimers were derived from RSV CA-NC (data not shown). In order to rule out the possibility that the multimers resulted from transient interactions because of high protein concentrations, this experiment was repeated with lower protein concentrations. The same cross-linking pattern was produced when the protein was serially diluted down to 0.05 mg/ml prior to the addition of EDC, suggesting that the CA-NC complexes are stable upon dilution (data not shown).

To determine whether CA-NC forms particles under these conditions, protein at 10 mg/ml was dialyzed overnight against

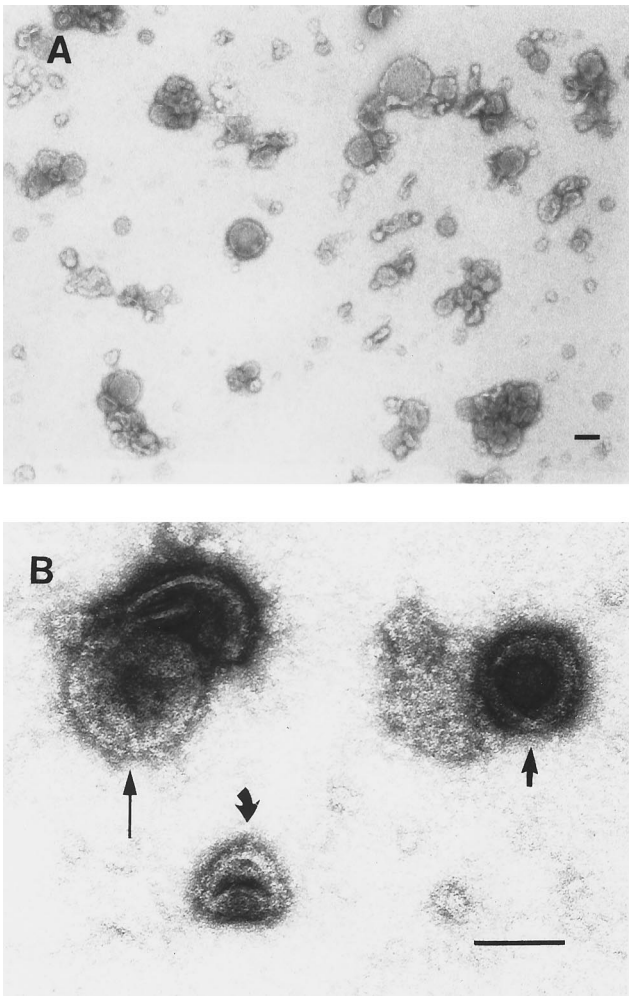

FIG. 3. Negative-stain EM image of RSV CA-NC assembled in vitro. (A) RSV CA-NC (10 mg/ml) in MES, pH 5.5, was negative stained with 2% uranyl acetate and examined by EM. (B) Higher magnification view showing a circular sheet (long arrow), a sheet with curled edges (curved arrow), and a spherical particle (short arrow). Bars, 100 nm.

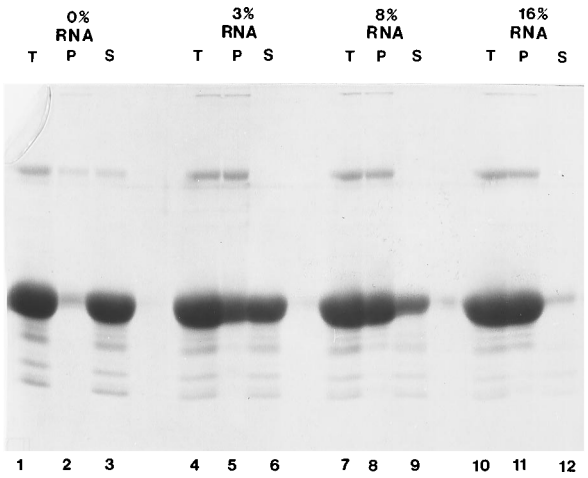

FIG. 4. Precipitation of RSV CA-NC with RNA. Total *E. coli* RNA was added to RSV CA-NC (1 mg/ml at pH 7.5, 0.5 M NaCl) at 0% (lanes 1 to 3), 3% (lanes 4 to 6), 8% (lanes 7 to 9), and 16% (lanes 10 to 12), wt/wt, RNA-protein prior to dialysis to 0.1 M NaCl, pH 5.5. The precipitates were pelleted by centrifugation in a microcentrifuge for 2 min. Equal proportions of the total (T), pellet (P), and supernatant (S) fractions were analyzed by SDS-PAGE and Coomassie blue staining.

the buffers used for cross-linking and then examined by EM after negative staining with uranyl acetate. No particulate material was observed at pH 8, as expected. By contrast, at pH 5.5 distinct structures were evident, consisting predominantly of what appeared to be flat, circular sheets or disks of heterogeneous size (Fig. 3A). Occasionally, cup-shaped objects and spherical particles were also seen (Fig. 3B), which might be produced by the curling up and fusing of the edges of the disk-shaped structures. The level of assembly efficiency decreased when either the pH or the NaCl concentration in the final dialysis step was increased. The self-assembled CA-NC particles could be collected by centrifugation for 1 h in a microcentrifuge (Fig. 4, lane 2), and they could also be purified by isopycnic banding in a 10 to 60% sucrose gradient (see Fig. 8A, lane 12). Both of these centrifugation procedures are used routinely to purify bona fide retrovirus particles. On the basis of the amount of protein recovered in the particulate fraction in these experiments, we estimate that only about 1% of the total protein assembled into particles. The significance of this low percentage is uncertain. However, the self-assembly that occurred appears to be a unique property of the CA-NC protein, since mature RSV CA and NC proteins, purified after digestion of CA-NC with AMV PR, did not assemble into these structures under any conditions tested, either alone or in combination with each other.

Since the NC domain of Gag interacts with the viral RNA during virion morphogenesis in vivo, we reasoned that RNA might affect the formation of particles in vitro. Total *E. coli* RNA was added to RSV CA-NC in a high salt concentration prior to dialysis. Within 15 min after the initiation of dialysis, a visible precipitate began to form. To investigate this phenomenon more quantitatively, we added various amounts of RNA to a constant amount of protein and then examined what proportion of the protein was in particles large enough to be collected by centrifugation for 2 min in a microcentrifuge (Fig. 4). The final amount of CA-NC in the pellet in this experiment was approximately proportional to the amount of RNA used (Fig. 4, compare lanes 2, 5, 8, and 11), i.e., in the range in which the mass ratio of RNA to protein varied from 0 to 16%. A similar experiment using from 12 to 60% (wt/wt) RNA failed to precipitate the remaining soluble protein seen in Fig. 4, lane 12 (data not shown). The remaining protein may be denatured, bound to small fragments of RNA, or otherwise unable to interact with the larger protein-RNA complex. Thus CA-NC appears to become saturated with RNA at between 8 and 12% RNA (wt/wt), corresponding to about 8 to 12 nt per molecule of CA-NC. This ratio is consistent with the stoichiometry of NC to RNA in the ribonucleoprotein complex isolated from virions (13), which corresponds to about 7 nt per NC molecule. It is also consistent with the saturation of RNA with purified NC measured in vitro for both RSV and MLV (32), or about 6 nt per molecule of NC. These comparisons suggest that the precipitate formed with RSV CA-NC and RNA involves interactions similar to those within the ribonucleoprotein complex in virions.

When examined by negative staining, the particles in the mixture of 3% RNA-protein showed multiple shapes. Structures similar to those formed without RNA were still visible but represented a minority of the particles. The majority were long cylindrical particles 30 nm in diameter and of varying lengths (Fig. 5A to C). Some cylinders were 50 nm in diameter, and these appeared to have an extra layer of protein over a

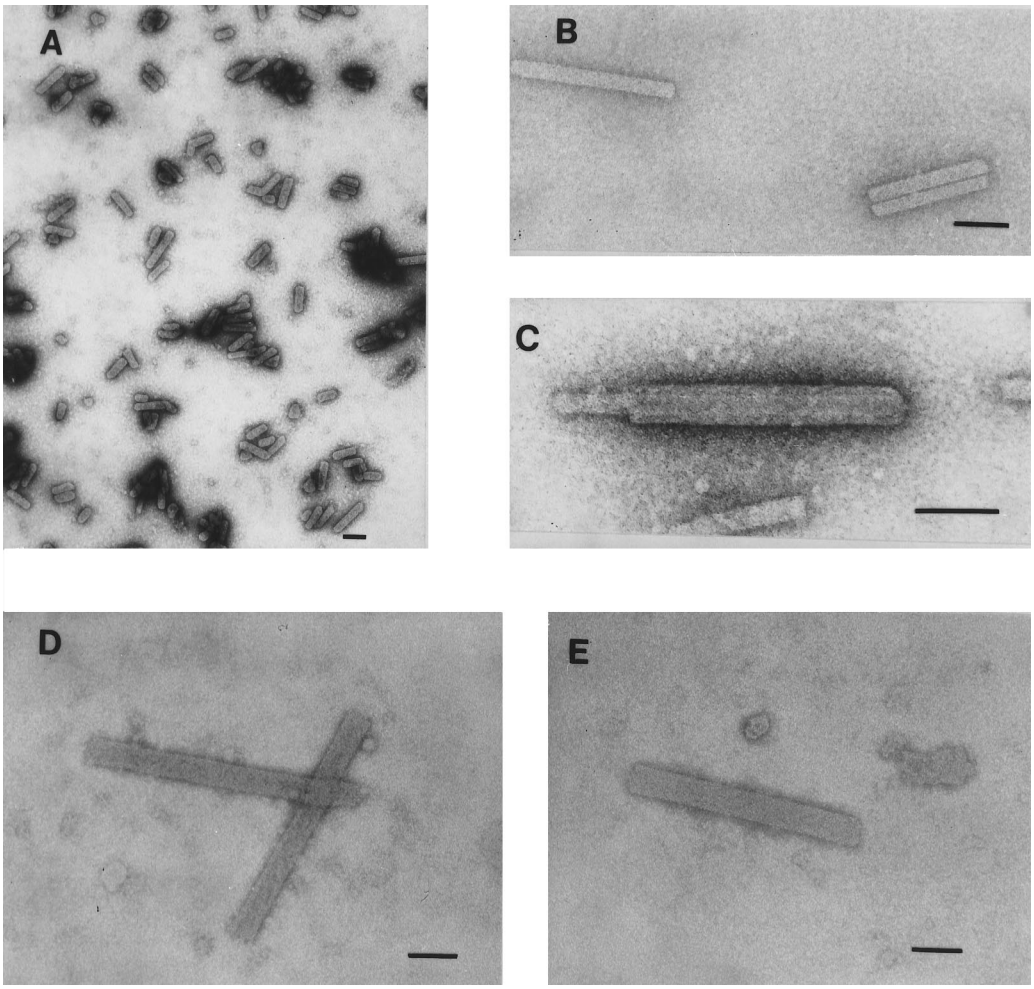

FIG. 5. Negative-stain EM image of RSV CA-NC, HIV CA-NC, and CA-NC-p6 assembled in vitro with *E. coli* RNA. RSV CA-NC (1 mg/ml) was dialyzed to pH 5.5 in the presence of 3% (wt/wt) *E. coli* RNA and negative stained with 2% uranyl acetate. Numerous rod-shaped particles of variable length but constant 30-nm diameter were observed (A and B). Occasional particles appeared to have a second layer of protein over a 30-nm core (C). HIV CA-NC (D) and CA-NC-p6 (E) also assembled into rod-shaped particles at pH 8.0 in the presence of RNA. The HIV particles were also of variable length but of constant 50-nm diameter. (D and E) Images were stained with phosphotungstic acid, pH 7.3. Bars, 100 nm.

30-nm core (Fig. 5C). Small, approximately spherical particles with a diameter of about 30 nm were commonly observed in initial experiments, but the production of these was not reproducible (see below). Large aggregates of particles were numerous (Fig. 6 and 7), which explains why the protein-RNA complexes were sedimentable by low-speed centrifugation. The aggregates predominated in reactions with RNA constituting more than 8% of the protein. Occasionally, particles that appeared to be in the process of assembling were visible (Fig. 6). These typically were connected to the aggregates by a strand of RNA covered with protein, suggesting that the RNA first becomes coated with CA-NC and then subsequently winds up in a helical fashion to form a cylinder.

If assembly proceeds in this manner, we hypothesized that, at least in part, the aggregates might result from the tangling of the protein-covered RNA strands. To test this idea, the aggregates were treated briefly with RNase for 10 min at 0.2 mg/ml. This treatment greatly increased the number of visible individual particles. However, continued incubation with RNase led to gradually shorter particles, until eventually they disappeared (data not shown). These results suggest that the small, roughly spherical particles observed with some preparations of CA-NC and RNA were due to contaminating RNase activity. To determine whether the CA and NC domains need to remain covalently attached for the maintenance of the cylindrical structure, we also digested particles with PR. After 2 h in assembly buffer at a wt/wt ratio of 1:100 PR/CA-NC, the visible precipitate cleared and particles were no longer detectable by negative staining. We also investigated the effects of nonionic detergent. Treatment with 0.01% Nonidet P-40 after assembly disrupted the cylindrical particles, but it did not seem to dissociate the protein from the RNA. Instead, what appeared to be large tangles of RNA covered with protein, with many small loops, were produced (data not shown), which resembled the structures observed after the disruption of Moloney MLV by freezing-thawing (45). For RSV as well as other retroviruses it is known that immature cores are stable in the presence of nonionic detergents after the removal of the lipid membrane, while, at least for most retroviruses, mature cores fall apart under the same conditions (58). The detergent sensitivity of the CA-NC particles thus makes them more similar in this regard to mature virions, suggesting that the MA domain contributes to detergent resistance in immature virions.

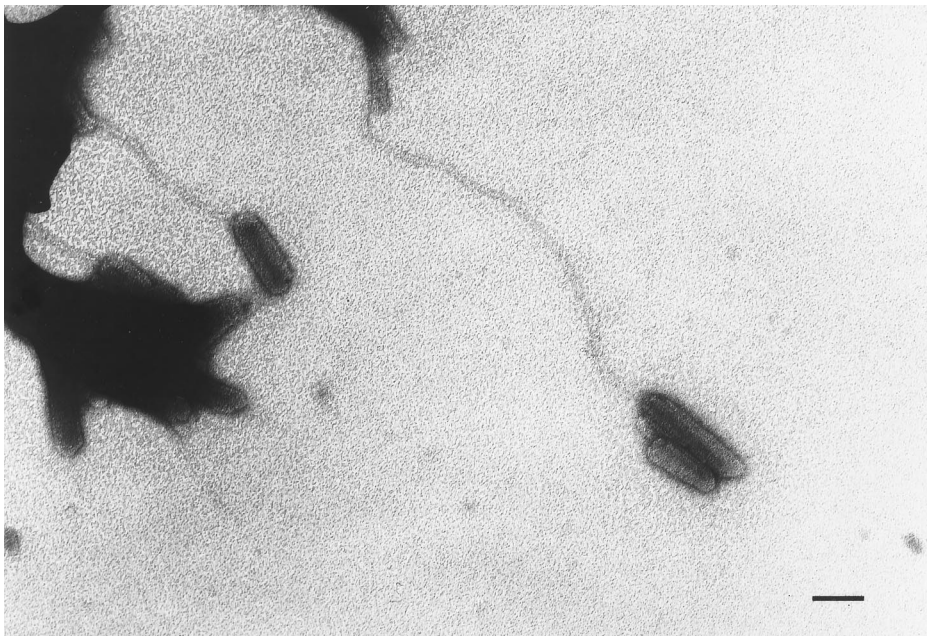

FIG. 6. Assembling RSV CA-NC-RNA particle. RSV CA-NC particles (lower right) assemble from strands of protein-coated RNA (center right) to form large aggregates of particles (upper left). The image was negative stained with 2% uranyl acetate. Bar, 100 nm.

To investigate if the formation of cylindrical particles by CA-NC and RNA represents an ability common to other retroviruses, we also used EM to examine the interaction of HIV CA-NC and HIV CA-NC-p6 with RNA. Incubations were carried out at pH 8.0 and pH 5.5 and 0.1 M NaCl, as for the RSV protein. Both HIV CA-NC and CA-NC-p6 also assembled into cylindrical particles in the presence of RNA, but this occurred only at the high pH (Fig. 5D and E), not at the low pH, as for

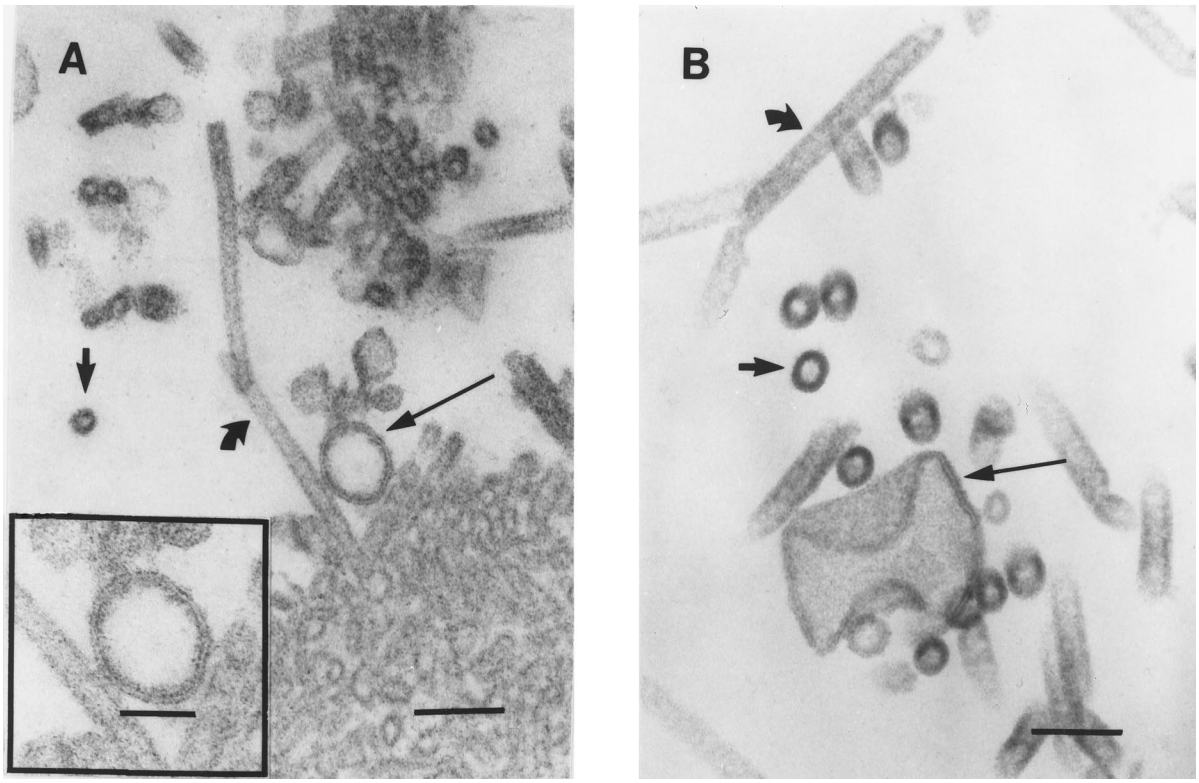

FIG. 7. Thin-section EM image of RSV and HIV particles. Thin sections of RSV CA-NC (A) and HIV CA-NC-p6 (B) particles formed with RNA; cross sections are indicated with short arrows and longitudinal sections are indicated with curved arrows. Structures interpreted as spherical particles or sheets formed without RNA were also present (long arrows in panels A and B and inset in panel A). Bars, 100 nm; 50 nm in inset.

TABLE 1. RNA length dependence of particle assembly[a]

RNA	Length of RNA (bases)	Length of particle (nm) (SD)	Length of RNA/length of particle (bases/nm) (SD)
CA-NC	2,735	137 (20)	20.4 (2.7)
D37N	3,575	171 (40)	22.0 (6.4)
TMV	6,395	298 (41)	21.9 (3.5)
AMV	~7,000	377 (60)	~18.6 (3.7)
Average			20.7
TMV[b]	6,395	304 (28)	21.2 (2.0)

[a] RSV CA-NC was assembled with either in vitro-translated RNA (CA-NC and D37N) or RNA purified from virions (TMV and AMV), and the length of the resulting particles was measured from photographic prints.

[b] Authentic TMV was included as a basis for comparison and as a control for the accuracy of the measurements.

RSV CA-NC. It is provocative that the HIV-1 CA protein itself is reported to polymerize into cylindrical structures at pH 6 and 1 M NaCl (17). Perhaps an increase in local concentration caused by binding to RNA, the presence of an unprocessed C terminus in the CA domain, or NC-NC interactions may cause CA-NC to form cylinders under conditions in which CA cannot.

The internal structure of the particles produced by the CA-NC proteins with and without RNA is not revealed by negative staining. In order to gain information about internal structure, we used thin sectioning after fixation and plastic embedding of a pellet of particles. The RSV CA-NC aggregates consisted almost entirely of assembled particles (Fig. 7A, bottom right), which had the appearance in cross section of hollow cylinders or tubes 25 to 30 nm in diameter with 10-nm-thick walls. The spherical particles produced without RNA also appeared hollow with 10-nm-thick walls, but the walls had a definite bilaminar appearance (Fig. 7A, inset). It is not clear whether the bilaminar appearance results from two distinct layers of protein separated by a gap or whether it represents only one layer of protein with a central, extended domain that is electron translucent. The walls of the tubes assembled with RNA were of the same thickness but did not seem to be bilaminar. Perhaps RNA fills this gap, or a conformational change occurs upon binding RNA to close this gap. The HIV-1 CA-NC-p6 and the HIV-1 CA-NC particles (Fig. 7B) were very similar in appearance to those of RSV CA-NC, except that the diameter was larger, being 50 to 60 nm. The bilaminar appearance of the circular sheets formed without RNA was also similar for HIV.

Taken together, the above results suggest that the length of the cylindrical particles is determined by the length of the RNA. To test this notion, RNAs of defined size were used for assembly with RSV CA-NC and measurements were made of a sampling of the resulting particles. A known cylindrical plant virus, tobacco mosaic virus (TMV), was included for comparison (9). The assembly reactions were performed with two types of RNA synthesized in vitro and with two types of virion RNA. The former consisted of RNAs corresponding to the CA-NC portion of the *gag* gene (2.7 kb) and to the entire *gag* gene (3.6 kb). The virion RNAs were from AMV (~7 kb) and from TMV (6.4 kb). We found that in all cases the average length of the particles was proportional to the length of the RNA (Table 1). The compaction ratio, i.e., the ratio of RNA length to particle length, was almost the same as the known ratio for TMV. The observation that the amount of variation in the lengths of the particles formed in vitro was considerably greater than the amount of variation in lengths of TMV itself could be attributed to the effects of RNase degradation during assembly, to incomplete assembly, or to end-to-end aggregation. We have not explored these possibilities experimentally.

The use of a bona fide virion RNA from a retrovirus closely related to RSV allowed us to address two issues in the in vitro assembly system, specificity and dimerization. In all retroviruses a packaging sequence near the 5′ end of the monomer directs the incorporation of genomic RNA into the virion. In the mature retrovirus the two identical copies of the genomic RNA form a dimer that is believed to be held together by hydrogen bonding of sequences near the packaging sequence. The time of dimer formation is unknown, but this process is thought to be intimately connected with assembly itself. We presumed that the saturated binding in vitro of CA-NC to any RNA results in the disruption of the RNA secondary structure and hence, in the case of the AMV RNA used here, also in the dissociation of the AMV RNA dimer. The observed lengths of the particles formed with AMV RNA is consistent with this idea, since the average size of the rods formed with the 14-kb dimeric AMV RNA was consonant with an RNA size of 7 kb. The observation that particle formation proceeded in a manner similar to that of AMV RNA, and all other RNAs, suggests that no specific RNA sequences are involved in this assembly system, at least under the particular conditions chosen.

Retroviruses have a characteristic density of about 1.16 to 1.18 as measured by isopycnic centrifugation in sucrose gradients. Immature viral cores, denuded of lipid by treatment with detergent or isolated from cells before budding (for viruses like M-PMV), have a higher density. To investigate this property for RSV CA-NC, we submitted the mixture of particles assembled in vitro to sedimentation in 10 to 60% sucrose gradients. The gradients were fractionated, and portions were analyzed by SDS-PAGE (Fig. 8) as well as by negative-stain EM. Authentic AMV (Fig. 8E) and TMV (Fig. 8D) were centrifuged in parallel. In the absence of RNA, most of the protein remained at the top of the gradient, but a minor turbid band visible by eye was present near the bottom with a density of approximately 1.20 g/ml. This fraction contained approximately 1% of the total CA-NC (Fig. 8A, lanes 11 and 12) and by EM showed the roughly spherical particles described above (not shown). With 12% (wt/wt) RNA-protein most of the protein pelleted to the bottom of the gradient as expected for aggregated particles (Fig. 8B, lanes 15 and 16). When a portion of the same reaction mixture was treated with RNase A for 10 min prior to sedimentation, some of the protein was released to the top of the gradient, but the remainder banded at the same density as the mixture with no RNA and as authentic TMV (Fig. 8C; compare lanes 11 and 12 with Fig. 8A and D). We conclude from these experiments that the aggregates can be dissociated into individual particles by RNase treatment. Interestingly, the cylindrical CA-NC particles and TMV banded at the same density as the spherical particles formed without RNA. By morphology and density the latter were very similar to the in vitro-assembled particles described by Klikova et al. (35) for M-PMV Gag, except that the RSV CA-NC particles were heterogeneous in size.

DISCUSSION

We have shown for two retroviruses that the purified CA-NC segment of the Gag protein is able to form particles in vitro. In the absence of RNA, assembly is inefficient and leads to a mixture of structures, some of which resemble spherical virions. In the presence of RNA, assembly is highly efficient and yields hollow, cylindrical structures. The regularity of the cylinders and their similarity in the two different viruses leads

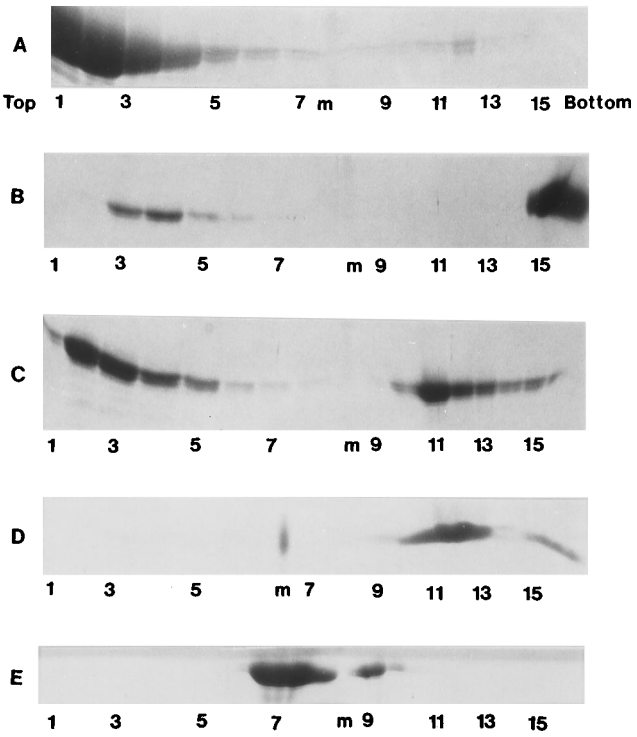

FIG. 8. Sucrose density gradient analysis. Coomassie blue-stained gel of sucrose density gradient fractions. Purified virus and assembled particles were layered on top of a 4-ml 10 to 60% linear sucrose gradient and centrifuged for 4 h at 50,000 rpm in a Beckman SW-60 rotor. After centrifugation, 16 equal fractions were collected, starting from the top of the tube, and analyzed by SDS-PAGE. RSV CA-NC assembled without RNA (A), with RNA (B), and with RNA but treated with RNase for 10 min prior to centrifugation (C). Purified TMV (D) and AMV (E) were centrifuged in parallel. Protein standards (lane m) were loaded onto the gel to identify lanes.

us to hypothesize that RNA plays a central role in the initiation and organization of virion formation in vivo.

We are aware of only one previous report of assembly of purified retroviral proteins (35). In that study the intact Gag protein of M-PMV was recovered from *E. coli* inclusion bodies solubilized in urea and was shown to form particles after removal of the urea by dialysis. The possible role of RNA in assembly was not carefully evaluated in that study. On the basis of negative staining, the particles were interpreted to be spherical and to resemble bona fide M-PMV capsids, but thin sectioning was not used to support this interpretation. It is thus possible that the M-PMV particles are more like the RSV CA-NC structures lacking RNA described here. This possibility is supported by our recent observation that an RSV Gag protein lacking only the PR domain also can assemble efficiently in vitro (9a). In that case the morphology of the structures formed in the absence of RNA is very similar to that of RNA-less CA-NC particles. Several factors might account for the apparent differences in the in vitro assembly efficiency (without RNA), or in morphology (in the presence of RNA), in RSV CA-NC and M-PMV Gag. First, the conditions for assembly in vitro are not identical. Second, D-type retroviruses like M-PMV preassemble their cores in the cytoplasm, while C-type viruses and lentiviruses like RSV and HIV-1, respectively, assemble at the site of budding on the plasma membrane. Finally, N-terminal domains, notably MA, were not present in the CA-NC proteins described here.

Little is known about the mechanisms for assembly of retroviruses in vivo and in particular about the role of RNA in this process. The pathways for formation of other spherical RNA viruses appear to fall into two categories (20). In one, viral proteins assemble first into distinct capsid intermediates, and then the genome is incorporated into one of these intermediates. In the other, viral proteins and RNA assemble into a complex that serves as a nucleation center for the continuous growth of the viral capsid in an RNA-dependent manner. It seems likely that retroviruses would fit into the latter category, since no distinct capsid intermediates have been observed, and by thin-section EM, C-type retroviruses do appear to assemble by a process of continuous growth. Clearly, however, there is no requirement for any specific viral sequences, since virions form normally in the absence of the packaging sequences that are located near the 5′ end of the best-studied retroviral RNAs (37–39, 54). This conclusion follows both from studies with transiently transfected cells and from studies with packaging cell lines used for the propagation of retroviral vectors in gene therapy. While virus particles produced in the absence of bona fide viral genomic RNA sometimes have been termed empty of RNA, in fact the possible role of nonspecific (host) RNA in assembly under these conditions has not been critically addressed in any retrovirus system.

How might the several structures formed in vitro by CA-NC proteins be interpreted in terms of observations on retrovirus assembly in vivo? In incubations of CA-NC without RNA, the most clearly discernible structures appeared to be circular, flattened sheets of heterogeneous size, some of which curled up to form cup-shaped or spherical particles. These sheets may be analogous to the electron-dense patches visible below the membrane in the assembly of C-type viruses. What may be similar curved sheets also have been observed within the cytoplasm of insect cells overexpressing HIV Gag protein with C-terminal deletions that lead to a reduced RNA binding ability (27, 31). It is difficult to interpret the low level of efficiency with which CA-NC forms regular structures in vitro. Presumably when the ionic conditions change during dialysis, there are competing reactions which the protein molecules can participate in, only some of which lead to distinct structures large enough to be remarkable by EM. Alternatively, there may be other essential components in the mixture that are present only in limiting quantities. These possibilities have not been explored experimentally.

In incubations of CA-NC with RNA, the RSV and HIV-1 proteins assembled into hollow cylinders of defined diameter but various lengths. Protein-covered strands of RNA seemed to wind up in a continuous fashion to form a helical cylinder. Cylindrical retrovirus particles also have been observed in vivo during budding, for M-PMV (60) and for certain HIV mutants (22, 26, 27). The particles budding from cells expressing an HIV mutant carrying a myristylation signal to replace the entire MA domain (i.e., essentially CA-NC-p6) were spherical (36). However, if present in the cells, cylindrical particles like those we have observed in vitro might easily have been mistaken for cytoskeletal elements.

We propose the following model to account for the cylindrical particles assembled in the presence of RNA (Fig. 9B, left). In this model RNA acts as a scaffold, an idea previously suggested for retrovirus assembly but without detail (22, 31, 68). CA-NC first binds to the RNA, as indicated by the ribonucleoprotein strands visible in Fig. 7. This binding may be due largely to electrostatic interactions of the multiple basic residues in NC with the negatively charged RNA backbone. Maximal packing of contiguous NC domains on the RNA, which may or may not be promoted by specific NC-NC interactions,

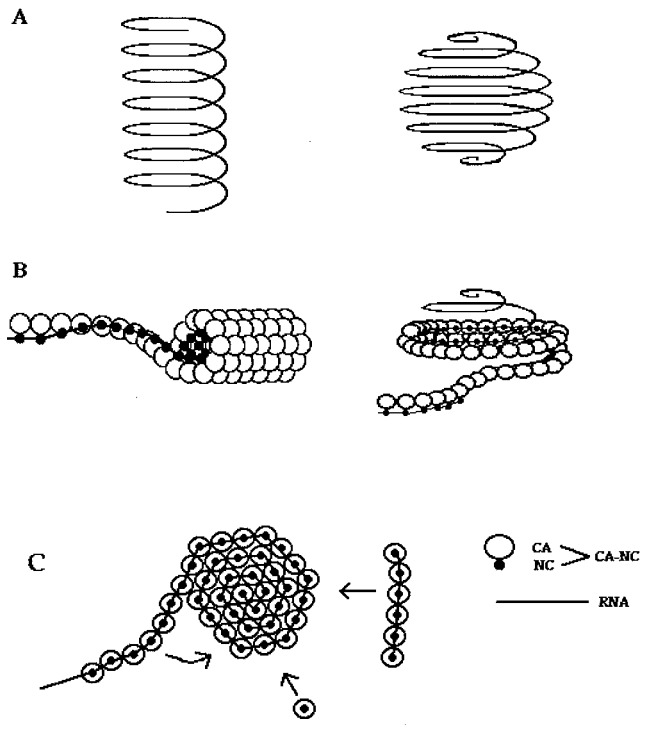

FIG. 9. Model for assembly of particles. A proposed model for the assembly of CA-NC and RNA into cylindrical particles in vitro or into spherical particles in vivo. The CA and NC domains are represented as spheres, and RNA is represented as an extended strand. (A) Comparison between a helical cylinder and a spiral sphere. (B) Comparison between CA-NC-RNA assembling into a cylinder (left) or possibly a spiral sphere (right). The protein first binds to RNA and then winds up to produce a particle. (C) View from within the cell illustrating the winding spiral and possible inclusion of individual proteins or proteins bound to small RNAs.

brings the CA domains close together. In the simplest version of the model, the differences in size of CA and NC play a role in inducing curvature of the strand. The closest packing of the small NC domains requires either that RNA bend to allow enough room for adjoining CA domains or that adjoining CA domains be offset. The ribonucleoprotein complex winds into a helix because of the side-to-side interactions between CA domains in neighboring loops of the helix. Assuming that each CA-NC molecule covers about 10 nt and that the RNA is fully extended and is inside as depicted, we estimate from the dimensions of the cylinder that each turn of the helix is composed of about 18 CA-NC molecules, compared with 16.3 protein subunits per turn for TMV (9), with the dimensions of each CA-NC molecule being approximately 2 by 3 by 10 nm. According to this model, the CA-CA interactions are weak and thus cylinder formation requires the local concentration of CA to be greatly elevated by the anchoring of the NC domain to an RNA molecule.

While the model is formulated to account for the in vitro assembly observed here, it should be applicable to the assembly of intact Gag proteins as well. Several predictions of the model are consistent with experimental findings on assembly in living cells. That the size of the CA domain may play a role in particle size is suggested by several deletion mutations in CA that result in larger than normal and heterogeneous particles (11, 14, 68). The contiguous packing of NC domains on the RNA is implied by the efficient formation of cross-links between NC domains upon treatment of an immature MLV-related virus, Gazdar sarcoma virus, with bifunctional reagents (48) and is consistent with the binding of NC to RNA in vitro (13, 32). Most important, it has been well established that the NC domain contains sequence elements indispensable for the assembly of particles with normal density in vivo (4, 30, 31, 68). This portion of NC, which in RSV is called AD3, probably comprises the two stretches of basic residues in this protein (1, 4, 42, 68a), at least one of which must be present for proper particle formation. AD3 also is the portion of Gag identified by deletion and complementation studies to be the locus of Gag-Gag interactions during budding (4, 31, 68, 70). The model suggests that Gag-Gag interactions in fact are mediated by RNA. Finally, the prediction that CA-CA interactions are weak is supported by the observations that the CA-NC cylinders formed in vitro are disrupted by low concentrations of nonionic detergent as well as by severing the CA-NC connection by digestion with PR.

The fact that CA-NC can form particles in vitro even in the absence of one-third of the Gag protein is consistent with roles that have been inferred for upstream and downstream sequences for assembly in cells. At the N terminus of Gag, the MA domain functions to transport and bind Gag to the plasma membrane (71, 73, 75) and to incorporate the envelope glycoproteins (66, 72) but is not itself needed for the formation of virus-like particles. (In some viruses MA also binds to RNA in vitro [33, 34, 57], but the biological significance of this binding is uncertain.) For example, in RSV a deletion of half of the MA domain, which prevents budding from transfected cells, can be efficiently suppressed by the N-terminal addition of a 10-amino-acid segment of the Src oncoprotein (71). HIV assembly still occurs, though with a reduced level of efficiency, if the entire MA domain is replaced by a glycine residue that allows myristylation (36). Similarly, much of the p2-p10 region of RSV between MA and CA can be deleted without affecting budding in transfected COS cells (69). The only essential portion of this part of Gag appears to include the conserved sequence PPPY and to function at the last stages of budding (45). In RSV the PR domain downstream of NC can be deleted without compromising budding in COS cells (67), although the same deletion in avian cells does reduce the level of efficiency of budding (59). In HIV, deletion of the p6 domain downstream of NC results in a late budding defect (25) similar to that caused by deletions in the p2 portion of RSV Gag. Indeed this late defect in RSV Gag can be corrected by the addition of the p6 domain of HIV (46). In any case, it is likely that, both in RSV and HIV, the aggregation of Gag proteins into a particulate structure is not affected by these mutations.

Cylindrical particles clearly are not normal forms for retroviruses. What clues are provided by the formation of such particles in vitro? It is conceptually simple to transform a cylindrical helix into a spherical spiral (Fig. 9A). Given the dimensions measured by EM (Table 1) and assuming an unchanged surface area, one could convert an RSV CA-NC particle formed with genomic viral RNA into a sphere with a diameter of about 100 nm, by equating the formulas for the surface areas of a cylinder and a sphere ($2\pi r_c h = 4\pi r_s^2$, where r_c is the radius of the cylinder, r_s is the radius of the sphere, and h is the length of the cylinder). This is approximately the diameter of a virion. Doubling the genome size to account for dimeric RNA still leaves the size within the range observed for retroviruses. Thus, it is possible that virion size may vary, within limits, according to the size of the RNA packaged and that the dimeric genome may provide the necessary amount of RNA required to organize a sufficient amount of Gag. Several small lengths of RNA could serve but are expected to be less efficient in this role than one long length. Recent data from

cryoelectron microscopy of HIV particles expressed in insect cells (20a) and MLV particles (35a) are consistent with the notion that virion size is not fixed tightly, in contrast to strictly icosahedral viruses like poliovirus, for example. We suggest that the association of Gag with the membrane confines assembly within two dimensions, thus favoring the assembly of spherical particles. In a speculative model of how this might occur (Fig. 9B, right and C), an RNA strand covered with Gag protein winds into a flat, circular spiral. Individual Gag proteins, or Gag bound to small strands of RNA, also could be incorporated without disturbing assembly. It is possible that the winding action of the RNA-Gag strand could serve to sweep up the viral envelope glycoprotein into the budding virion, either through direct interaction or by displacing cellular membrane proteins. Simultaneously with the winding up of the protein-RNA strand, the protein-protein and protein-RNA interactions proposed above would induce curvature to push the budding virion out of the plasma membrane. While the formation of cylinders might be possible, as observed with some mutants, the formation of spheres would involve the least distortion of the membrane and thus be favored. An obvious prediction of this model is that the RNA in the newly budded virion is not radially symmetrical.

It is well known that proteins making up simple macromolecular structures with repeating units often are capable of forming alternative repeating structures. The subunit contacts in a sheet and in an icosahedron are expected to be very similar. Thus, the protein-protein and protein-RNA interactions in the cylinders we have observed in vitro are also likely to be very similar to those interactions in bona fide spherical virions. Perhaps the most relevant example of a viral protein capable of polymerizing into alternative structures is the capsid protein of cowpea chlorotic mosaic virus, which was shown more than 20 years ago to be able in vitro to form T=1 icosahedra, T=3 icosahedra, sheets, and cylinders, depending on the conditions of pH, salt, and the presence or absence of RNA (3). Indeed, the tubes formed by cowpea chlorotic mosaic virus bear remarkable resemblance to the cylindrical particles we have observed here. The three-dimensional structure of this virus has recently been characterized in detail, using crystallography and cryoelectron microscopy (56), and in some respects might serve as a model for retroviruses. The important features of the cylindrical particles of RSV and HIV CA-NC may be able to be unraveled by means of cryoelectron microscopy. However, detailed interpretations of EM data will require knowledge of the three-dimensional structures of the individual proteins. While NMR structures of HIV NC (44) and HIV MA (40, 41) have been reported, no structure is yet available for CA. However, crystallographic work on HIV CA as well as on RSV CA is in progress (52, 52a). The in vitro assembly system described here may be an important tool to help understand the principles of retrovirus assembly.

ACKNOWLEDGMENTS

We acknowledge the work of Paul Mason, who subcloned the HIV-1 CA-NC and CA-NC-p6 constructs from the BH10 clone of HIV-1, supplied by Hans-Georg Kräusslich, and who performed the first purification and first assembly experiments with these proteins. We thank Milton Zaitlin for the gift of TMV and Jack Johnson for pointing out the similarities with cowpea chlorotic mosaic virus and for encouragement and helpful comments on this project. We also thank John Wills for comments and enthusiastic encouragement.

This work was supported by USPHS grant CA-20081.

ADDENDUM IN PROOF

A model for the assembly of C type retroviruses in some respects similar to the one discussed here was proposed in 1971. N. H. Sarkar, R. C. Nowinski, and D. H. Moore. J. Virol. **8:**564–572, 1971).

REFERENCES

1. **Aronoff, R., A. M. Hajjar, and M. L. Linial.** 1993. Avian retroviral RNA encapsidation: reexamination of functional 5′ RNA sequences and the role of nucleocapsid Cys-His motifs. J. Virol. **67:**178–188.
2. **Ausubel, F. M.** 1994. Current protocols in molecular biology. Preparation and analysis of RNA. John Wiley & Sons, Inc., New York.
3. **Bancroft, J. B.** 1970. The self-assembly of spherical plant viruses. Adv. Virus Res. **16:**99–134.
4. **Bennett, R. P., T. D. Nelle, and J. W. Wills.** 1993. Functional chimeras of the Rous sarcoma virus and human immunodeficiency virus Gag proteins. J. Virol. **67:**6487–6498.
5. **Berkowitz, R. D., and S. P. Goff.** 1994. Analysis of binding elements in the human immunodeficiency virus type 1 genomic RNA and nucleocapsid protein. Virology **202:**233–246.
6. **Berkowitz, R. D., J. Luban, and S. P. Goff.** 1993. Specific binding of human immunodeficiency virus type 1 Gag polyprotein and nucleocapsid protein to viral RNAs detected by RNA mobility shift assays. J. Virol. **67:**7190–7200.
7. **Bowles, N. E., P. Damay, and P.-F. Spahr.** 1993. Effect of rearrangements and duplications of the Cys-His motifs of Rous sarcoma virus nucleocapsid protein. J. Virol. **67:**623–631.
8. **Burns, N. R., S. Craig, S. R. Lee, S. M. H. Richardson, N. Stenner, S. E. Adams, S. M. Kingsman, and A. J. Kingsman.** 1990. Purification and secondary structure determination of simian immunodeficiency virus p27. J. Mol. Biol. **216:**207–211.
9. **Butler, P. J. G.** 1984. The current picture of the structure and assembly of tobacco mosaic virus. J. Gen. Virol. **65:**253–279.

9a. **Campbell, S., and V. Vogt.** Unpublished observations.

10. **Carriere, C., B. Gay, N. Chazal, N. Morin, and P. Boulanger.** 1995. Sequence requirements for encapsidation of deletion mutants and chimeras of human immunodeficiency virus type 1 Gag precursor into retrovirus-like particles. J. Virol. **69:**2366–2377.
11. **Chazal, N., C. Carriere, B. Gay, and P. Boulanger.** 1994. Phenotypic characterization of insertion mutants of the human immunodeficiency virus type 1 Gag precursor expressed in recombinant baculovirus-infected cells. J. Virol. **68:**111–122.
12. **Dannull, J., A. Surovoy, G. Jung, and K. Moelling.** 1994. Specific binding of HIV-1 nucleocapsid protein to PSI RNA in vitro requires N-terminal zinc finger and flanking basic amino acid residues. EMBO J. **13:**1525–1533.
13. **Davis, N. L., and R. R. Rueckert.** 1972. Properties of a ribonucleoprotein particle isolated from Nonidet P-40-treated Rous sarcoma virus. J. Virol. **10:**1010–1020.
14. **Dorfman, T., A. Bukovsky, A. Ohagen, S. Hoglund, and H. G. Gottlinger.** 1994. Functional domains of the capsid protein of human immunodeficiency virus type 1. J. Virol. **68:**8180–8187.
15. **Dorfman, T., J. Luban, S. P. Goff, W. A. Haseltine, and H. G. Gottlinger.** 1993. Mapping of functionally important residues of a cysteine-histidine box in the human immunodeficiency virus type 1 nucleocapsid protein. J. Virol. **67:**6159–6169.
16. **Dupraz, P., S. Oertle, C. Méric, P. Damay, and P.-F. Spahr.** 1990. Point mutations in the proximal Cys-His box of Rous sarcoma virus nucleocapsid protein. J. Virol. **64:**4978–4987.
17. **Ehrlich, L. S., B. E. Agresta, and C. A. Carter.** 1992. Assembly of recombinant human immunodeficiency virus type 1 capsid protein in vitro. J. Virol. **66:**4874–4883.
18. **Ehrlich, L. S., B. E. Agresta, C. A. Gelfand, J. Jentoft, and C. A. Carter.** 1994. Spectral analysis and tryptic susceptibility as probes of HIV-1 capsid protein structure. Virology **204:**515–525.
19. **Fäcke, M., A. Janetzko, R. L. Shoeman, and H.-G. Kräusslich.** 1993. A large deletion in the matrix domain of the human immunodeficiency virus *gag* gene redirects virus particle assembly from the plasma membrane to the endoplasmic reticulum. J. Virol. **67:**4972–4980.
20. **Fox, J. M., J. E. Johnson, and M. J. Young.** 1994. RNA/protein interactions in icosahedral virus assembly. Semin. Virol. **5:**51–60.

20a. **Fuller, S., and V. Vogt.** Unpublished data.

21. **Gelderblom, H. R., E. H. S. Hausmann, M. Ozel, G. Pauli, and M. A. Koch.** 1987. Fine structure of human immunodeficiency virus (HIV) and immunolocalization of structural protein. Virology **156:**171–176.
22. **Gheysen, D., E. Jacobs, F. de Foresta, C. Thiriart, M. Francotte, D. Thines, and M. De Wilde.** 1989. Assembly and release of HIV-1 precursor $Pr55^{gag}$ virus-like particles from recombinant baculovirus-infected insect cells. Cell **59:**103–112.
23. **Gorelick, R. J., D. J. Chabot, A. Rein, L. E. Henderson, and L. O. Arthur.** 1993. The two zinc fingers in the human immunodeficiency virus type 1 nucleocapsid protein are not functionally equivalent. J. Virol. **67:**4027–4036.

24. **Gorelick, R. J., S. M. J. Nigida, J. W. J. Bess, L. O. Arthur, L. E. Henderson, and A. Rein.** 1990. Noninfectious human immunodeficiency virus type 1 mutants deficient in genomic RNA. J. Virol. **64:**3207–3211.
25. **Göttlinger, H. G., T. Dorfman, J. G. Sodroski, and W. A. Haseltine.** 1991. Effect of mutations affecting the p6 gag protein on human immunodeficiency virus particle release. Proc. Natl. Acad. Sci. USA **88:**3195–3199.
26. **Göttlinger, H. G., J. G. Sodroski, and W. A. Haseltine.** 1989. Role of capsid precursor processing and myristoylation in morphogenesis and infectivity of human immunodeficiency virus type 1. Proc. Natl. Acad. Sci. USA **86:**5781–5785.
27. **Hockley, D. J., M. V. Nermut, C. Grief, J. B. M. Jowett, and I. M. Jones.** 1994. Comparative morphology of Gag protein structures produced by mutants of the gag gene of human immunodeficiency virus type 1. J. Gen. Virol. **75:**2985–2997.
28. **Hunter, E.** 1994. Macromolecular interactions in the assembly of HIV and other retroviruses. Semin. Virol. **5:**71–83.
29. **Johnson, S. P., M. Veigl, T. Vanaman, and J. Leis.** 1983. Cyanogen bromide digestion of avian myoblastosis virus pp19 protein: isolation of an amino-terminal peptide that binds RNA. J. Virol. **45:**876–881.
30. **Jones, T. A., G. Blaug, M. Hansen, and E. Barklis.** 1990. Assembly of *gag*-β-galactosidase proteins into retrovirus particles. J. Virol. **64:**2265–2279.
31. **Jowett, J. B. M., D. J. Hockley, M. V. Nermut, and I. M. Jones.** 1992. Distinct signals in human immunodeficiency virus type 1 Pr55 necessary for RNA binding and particle formation. J. Gen. Virol. **73:**3079–3086.
32. **Karpel, R. L., L. E. Henderson, and S. Oroszlan.** 1987. Interactions of retroviral structural proteins with single-stranded nucleic acids. J. Biol. Chem. **262:**4961–4967.
33. **Katoh, I., H. Kyushiki, Y. Sakamoto, Y. Ikawa, and Y. Yoshinaka.** 1991. Bovine leukemia virus matrix-associated protein MA (p15): further processing and formation of a specific complex with the dimer of the 5′-terminal genomic RNA fragment. J. Virol. **65:**6845–6855.
34. **Katoh, I., T. Yasunaga, and Y. Yoshinaka.** 1993. Bovine leukemia virus RNA sequences involved in dimerization and specific *gag* protein binding: close relation to the packaging sites of avian, murine, and human retroviruses. J. Virol. **67:**1830–1839.
35. **Klikova, M., S. S. Rhee, E. Hunter, and T. Ruml.** 1995. Efficient in vivo and in vitro assembly of retroviral capsids from Gag precursor proteins expressed in bacteria. J. Virol. **69:**1093–1098.

35a. **Kubalick, E.** Personal communication.

36. **Lee, P. P., and M. L. Linial.** 1994. Efficient particle formation can occur if the matrix domain of human immunodeficiency virus type 1 Gag is substituted by a myristylation signal. J. Virol. **68:**6644–6654.
37. **Levin, J. G., P. M. Grimley, J. M. Ramseur, and I. K. Berezesky.** 1974. Deficiency of 60 to 70S RNA in murine leukemia virus particles assembled in cells treated with actinomycin D. J. Virol. **14:**152–161.
38. **Linial, M., E. Medeiros, and W. S. Hayward.** 1978. An avian oncovirus mutant (SE21Q1b) deficient in genomic RNA: biological and biochemical characterization. Cell **15:**1371–1381.
39. **Linial, M. L., and A. D. Miller.** 1990. Retroviral RNA packaging: sequence requirements and implications. Curr. Top. Microbiol. Immunol. **157:**125–152.
40. **Massiah, M. A., M. R. Starich, C. M. Paschall, M. F. Summers, A. M. Christensen, and W. I. Sundquist.** 1994. Three-dimensional structure of the human immunodeficiency virus type 1 matrix protein. J. Mol. Biol. **244:**194–223.
41. **Matthews, S., P. Barlow, J. Boyd, G. Barton, R. Russell, H. Mills, M. Cunningham, N. Meyers, N. Burns, N. Clark, S. Kingsman, A. Kingsman, and I. Campbell.** 1994. Structural similarity between the p17 matrix protein of HIV-1 and interferon-γ. Nature (London) **370:**666–668.
42. **Méric, C., E. Gouilloud, and P.-F. Spahr.** 1988. Mutations in Rous sarcoma virus nucleocapsid protein p12 (NC): deletions of Cys-His boxes. J. Virol. **62:**3328–3333.
43. **Méric, C., and P.-F. Spahr.** 1986. Rous sarcoma virus nucleic acid-binding protein p12 is necessary for viral 70S RNA dimer formation and packaging. J. Virol. **60:**450–459.
44. **Morellet, N., N. Jullian, H. De Rocquigny, B. Maigret, J.-L. Darlix, and B. P. Roques.** 1992. Determination of the structure of the nucleocapsid protein NCp7 from the human immunodeficiency virus type 1 by ^{1}H NMR. EMBO J. **11:**3059–3065.
45. **Pager, J., D. Coulaud, and E. Delain.** 1994. Electron microscopy of the nucleocapsid from disrupted Moloney murine leukemia virus and of associated type VI collagen-like filaments. J. Virol. **68:**223–232.
46. **Parent, L. J., R. P. Bennet, R. C. Craven, T. D. Nelle, N. K. Krishna, J. B. Bowzard, C. B. Wilson, B. A. Puffer, R. C. Montelaro, and J. W. Wills.** Positionally independent and exchangeable late budding functions of the Rous sarcoma virus and human immunodeficiency virus Gag proteins. J. Virol. **69:**5455–5460.
47. **Pepinsky, R. B., and V. M. Vogt.** 1979. Identification of retrovirus matrix proteins by lipid-protein cross-linking. J. Mol. Biol. **131:**819–837.
48. **Pepinsky, R. B.** 1983. Localization of lipid-protein and protein-protein interactions within the murine retrovirus gag precursor by a novel peptide-mapping technique. J. Biol. Chem. **258:**11229–11235.

48a. **Pepinsky, R. B.** Personal communication.

49. **Pepinsky, R. B., D. Cappiello, C. Wilkowski, and V. M. Vogt.** 1980. Chemical crosslinking of proteins in avian sarcoma and leukemia viruses. Virology **102:**205–210.
50. **Pepinsky, R. B., and V. M. Vogt.** 1984. Fine-structure analyses of lipid-protein and protein-protein interactions of Gag protein p19 of the avian sarcoma and leukemia viruses by cyanogen bromide mapping. J. Virol. **52:**145–153.
51. **Pognonec, P., H. Kato, H. Sumimoto, M. Kretzschmer, and R. G. Roeder.** 1991. A quick procedure for purification of functional recombinant proteins over-expressed in *E. coli*. Nucleic Acids Res. **19:**6650.
52. **Prongay, A. J., T. J. Smith, M. G. Rossmann, L. S. Ehrlich, C. A. Carter, and J. McClure.** 1990. Preparation and crystallization of a human immunodeficiency virus p24-Fab complex. Proc. Natl. Acad. Sci. USA **87:**9980–9984.

52a. **Rossmann, M.** Personal communication.

53. **Sakalian, M., J. W. Wills, and V. M. Vogt.** 1994. Efficiency and selectivity of RNA packaging by Rous sarcoma virus Gag deletion mutants. J. Virol. **68:**5969–5981.
54. **Schlesinger, S., S. Makino, and M. L. Linial.** 1994. Cis-acting genomic elements and trans acting proteins involved in the assembly of RNA viruses. Semin. Virol. **5:**39–49.
55. **Schwartz, D. E., R. Tizard, and W. Gilbert.** 1983. Nucleotide sequence of Rous sarcoma virus. Cell **32:**853–869.
56. **Speir, J. A., M. Sanjeev, G. Wang, T. S. Baker, and J. E. Johnson.** 1995. Structures of the native and swollen forms of cowpea chlorotic mottle virus determined by X-ray crystallography and cryo-electron microscopy. Structure **3:**63–78.
57. **Steeg, C. M., and V. M. Vogt.** 1990. RNA-binding properties of the matrix protein ($p19^{gag}$) of avian sarcoma and leukemia viruses. J. Virol. **64:**847–855.
58. **Stewart, L., G. Schatz, and V. M. Vogt.** 1990. Properties of avian retrovirus particles defective in viral protease. J. Virol. **64:**5076–5092.
59. **Stewart, L., and V. M. Vogt.** 1991. *trans*-acting viral protease is necessary and sufficient for activation of avian leukosis virus reverse transcriptase. J. Virol. **65:**6218–6231.
60. **Strambio-de-Castillia, C., and E. Hunter.** 1992. Mutational analysis of the major homology region of Mason-Pfizer monkey virus by use of saturation mutagenesis. J. Virol. **66:**7021–7032.
61. **Studier, F. W., and B. A. Moffat.** 1986. Use of bacteriophage T7 RNA polymerase to direct selective high-level expression of cloned genes. J. Mol. Biol. **189:**113–130.
62. **Studier, F. W., A. H. Rosenberg, J. J. Dunn, and J. W. Dubendorff.** 1990. Use of T7 RNA polymerase to direct expression of cloned genes. Methods Enzymol. **185:**60–89.
63. **Surovoy, A., J. Dannull, K. Moelling, and G. Jung.** 1993. Conformation and nucleic acid binding studies on the synthetic nucleocapsid protein of HIV-1. J. Mol. Biol. **229:**94–104.
64. **Wagner, R., L. Deml, H. Fliessbach, G. Wanner, and H. Wolf.** 1994. Assembly and extracellular release of chimeric HIV-1 $Pr55^{gag}$ retrovirus-like particles. Virology **200:**162–175.
65. **Wang, C.-T., and E. Barklis.** 1993. Assembly, processing, and infectivity of human immunodeficiency virus type 1 Gag mutants. J. Virol. **67:**4264–4273.
66. **Wang, C.-T., Y. Zhang, J. McDermott, and E. Barklis.** 1993. Conditional infectivity of a human immunodeficiency virus matrix domain deletion mutant. J. Virol. **67:**7067–7076.
67. **Weldon, R. A., Jr., C. R. Erdie, M. G. Oliver, and J. W. Wills.** 1990. Incorporation of chimeric Gag protein into retroviral particles. J. Virol. **64:**4169–4179.
68. **Weldon, R. A., Jr., and J. W. Wills.** 1993. Characterization of a small (25-kilodalton) derivative of the Rous sarcoma virus Gag protein competent for particle release. J. Virol. **67:**5550–5561.

68a. **Wills, J.** Personal communication.

69. **Wills, J. W., C. E. Cameron, C. B. Wilson, Y. Xiang, R. P. Bennett, and J. Leis.** 1994. An assembly domain of the Rous sarcoma virus Gag protein required late in budding. J. Virol. **68:**6605–6618.
70. **Wills, J. W., and R. C. Craven.** 1991. Form, function, and use of retroviral Gag proteins. AIDS **5:**639–654.
71. **Wills, J. W., R. C. Craven, R. A. Weldon, Jr., T. D. Nelle, and C. R. Erdie.** 1991. Suppression of retroviral MA deletions by the amino-terminal membrane-binding domain of $p60^{src}$. J. Virol. **65:**3804–3812.
72. **Yu, X., X. Yuan, Z. Matsuda, T.-H. Lee, and M. Essex.** 1992. The matrix protein of human immunodeficiency virus type 1 is required for incorporation of viral envelope protein into mature virions. J. Virol. **66:**4966–4971.
73. **Yuan, X., X. Yu, T.-H. Lee, and M. Essex.** 1993. Mutations in the N-terminal region of human immunodeficiency virus type 1 matrix protein block intracellular transport of the Gag precursor. J. Virol. **67:**6387–6394.
74. **Zhao, Y., I. M. Jones, D. J. Hockley, M. V. Nermut, and P. Roy.** 1994. Complementation of human immunodeficiency virus (HIV-1) Gag particle formation. Virology **199:**403–408.
75. **Zhou, W., L. J. Parent, J. W. Wills, and M. D. Resh.** 1994. Identification of a membrane-binding domain within the amino-terminal region of human immunodeficiency virus type 1 Gag protein which interacts with acidic phospholipids. J. Virol. **68:**2556–2569.